

Patent Abstracts of Japan

PUBLICATION NUMBER : 02238659
PUBLICATION DATE : 20-09-90

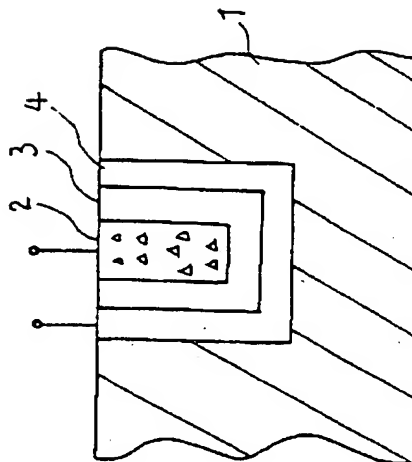
APPLICATION DATE : 10-03-89
APPLICATION NUMBER : 01058912

APPLICANT : SEIKO EPSON CORP;

INVENTOR : IWAMATSU SEIICHI;

INT.CL. : H01L 27/102 H01L 29/91

TITLE : DYNAMIC MEMORY ELEMENT



ABSTRACT : PURPOSE: To realize a high speed and a high integration of a memory element by a method wherein a diode structure provided with a junction is formed on side walls of a hill-shaped or trenchshaped semiconductor.

CONSTITUTION: A trench is formed from the surface of an Si substrate 1; an n-type diffusion layer 34 and a P-type diffusion layer 23 are formed of the trench part; an n-type polycrystalline Si layer is filled into the trench part to form a diffusion layer 12. A dynamic memory action is made possible by means of a two-pole n-p-n structure diode by the diffusion layer 12 and the diffusion layer 34. Thereby, a diode-type dynamic memory element of a bipolar type can be realized; a high speed and a high integration of a memory can be realized.

COPYRIGHT: (C)1990,JPO&Japio

THIS PAGE BLANK (USPTO)

⑩ 日本国特許庁(JP)

⑪ 特許出願公開

⑫ 公開特許公報(A)

平2-238659

⑬ Int. Cl.³

識別記号

庁内整理番号

⑭ 公開 平成2年(1990)9月20日

H 01 L 27/102
29/91

8624-5F H 01 L 27/10 3 3 1
7638-5F 29/91 C

審査請求 未請求 請求項の数 1 (全2頁)

⑮ 発明の名称 ダイナミックメモリ素子

⑯ 特 願 平1-58912

⑰ 出 願 平1(1989)3月10日

⑱ 発 明 者 岩 松 誠 一 長野県諏訪市大和3丁目3番5号 セイコーエプソン株式会社内

⑲ 出 願 人 セイコーエプソン株式会社 東京都新宿区西新宿2丁目4番1号

⑳ 代 理 人 弁理士 鈴木 喜三郎 外1名

明 細 書

1 発明の名称

ダイナミック メモリ素子

2 特許請求の範囲

少なくとも山型又はトレンチ型半導体の側壁に接合を有するダイオード構造となす事を特徴とするダイナミック メモリ素子。

3 発明の詳細な説明

[産業上の利用分野]

本発明はバイポーラ型の新しい2電極式ダイナミック メモリ素子構造に関する。

[従来の技術]

従来、ダイナミック メモリ素子としてはコンデンサ蓄積型のMOS FETを利用したダイナミック メモリ素子は有ったが、バイポーラ型のダイナミック メモリ素子はなかった。

[発明が解決しようとする課題]

しかし、上記従来技術によると、高速化や高集積化を計る事が困難であると云う課題があった。

本発明はかかる従来技術の課題を解決し、バイポーラ型のダイオード型ダイナミック メモリ素子と云う新しい構造を提案し、メモリ素子の高速化と高集積化を可能とする事を目的とする。

[課題を解決するための手段]

上記課題を解決するために、本発明は、ダイナミック メモリ素子に関し、少なくとも山型又はトレンチ型半導体の側壁に、接合を有するダイオード構造となす手段をとる。

[実施例]

以下、実施例により本発明を詳述する。

第1図及び第2図は、本発明の実施例を示す、ダイナミック メモリ素子の断面図である。

第1図では、S1基板1の表面からトレンチを形成して、該トレンチ部からn型の拡散層(3)4、

(1)

(2)

p型の拡散層(2)3を形成し、前記トレンチ部にn型多結晶S1層を埋め込んで拡散層(1)2となしたもので、拡散層(1)2と拡散層(3)4との2極のnpn構造ダイオードにてダイナミックメモリ作用が可能なものである。

第2図では、i(Intinsic)型GaAs基板11の表面にGaAsから成るn型のエピタキシャル層(1)12を形成し、該n型のエピタキシャル層(1)12の一部を山型となし、更にその表面に、i層(1)13、p型のエピタキシャル層(2)14、i層(2)15、n型のエピタキシャル層(3)16をGaAsにて積層して形成し、エピタキシャル層(1)12とエピタキシャル層(3)16を2極となした、npin構造のダイオード型のダイナミックメモリ素子である。尚、山型はi型のGaAs基板11に予じめ形成しておいても良い。

〔発明の効果〕

本発明によりバイポーラ型のダイオード型ダイナミックメモリ素子が提供でき、メモリの高速

化及び高集積化を計る事ができる効果がある。

4. 図面の簡単な説明

第1図及び第2図は、本発明の実施例を示すダイナミックメモリ素子の断面図である。

1 …… Si基板

2 …… 拡散層(1)

3 …… 拡散層(2)

4 …… 拡散層(3)

11 …… GaAs基板

12 …… エピタキシャル層(1)

13 …… i層(1)

14 …… エピタキシャル層(2)

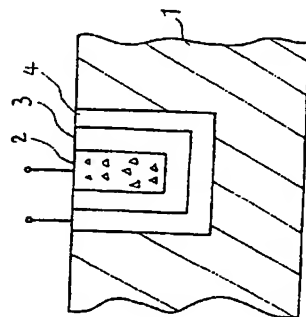
15 …… i層(2)

16 …… エピタキシャル層(3)

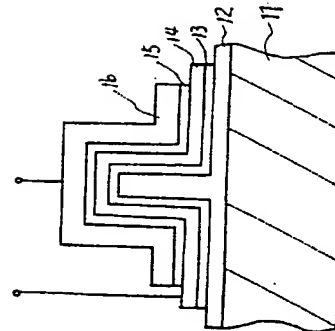
以上

出願人 セイコーエプソン株式会社

代理人 弁理士 上柳雅幸(他1名)



第1図



第2図

Electronic transport and magnetic properties in $(\text{La}_{1-x}\text{Gd}_x)_{0.67}\text{Ca}_{0.33}\text{MnO}_3$ perovskites

J.H. Hao ^{a,*}, Z.S. Li ^b, H.K. Wong ^c

^a Department of Optoelectronic Engineering, Huazhong University of Science and Technology, Wuhan 430074, People's Republic of China

^b Magnet Laboratory, Massachusetts Institute of Technology, Cambridge, MA 02139, USA

^c Physics Department, The Chinese University of Hong Kong, Hong Kong, People's Republic of China

Received 9 May 2000; accepted 1 December 2000

Abstract

Polycrystalline samples of La-Ca-Mn-O doped with Gd have been prepared. We have systematically examined their electronic transport, low-field magnetoresistance, and magnetization behaviors in a series of $(\text{La}_{1-x}\text{Gd}_x)_{0.67}\text{Ca}_{0.33}\text{MnO}_3$ with $0.10 \leq x \leq 1.00$. The maximum magnetoresistance ratio at $B = 0.85$ T with $(R_0 - R_B)/R_0 = 92.5\%$ occurs approximately at $x = 0.3$. It is also found that the Gd-doped samples show a novel memory effect. The effects of gadolinium ion composition on the electric and magnetoresistance behaviors of manganese perovskites $(\text{La}_{1-x}\text{Gd}_x)_{0.67}\text{Ca}_{0.33}\text{MnO}_3$ could arise as from changes in the average ionic radius of the La site $\langle r_A \rangle$. © 2001 Elsevier Science B.V. All rights reserved.

Keywords: Colossal magnetoresistance; Transport; Magnetic; Manganese perovskite; Memory effect

1. Introduction

The complex perovskite compounds $\text{La}_{1-x}\text{A}_x\text{MnO}_3$ ($\text{A} = \text{Ca}, \text{Sr}, \text{Ba}$ and Pb) can be formed and exhibit very interesting magnetic and electrical properties when La is partially substituted by divalent elements [1]. The most attractive feature of their behavior is the existence of metallic conductivity and ferromagnetism.

There is renewed interest in manganese perovskites due to their colossal magnetoresistance (CMR) effect exhibited near the ferromagnetic ordering of Mn spins [2–5]. The MR ratio is defined here as $\Delta R/R_0 = (R_0 - R_B)/R_0$ where R_0 is the zero-field electrical resistance and R_B is the resistance in the applied field. The reported MR value are 60% at 7 T and 300 K in $\text{La}_{0.67}\text{Ba}_{0.33}\text{MnO}_3$ thin films [4], 99.9% at 6 T and 77 K in an epitaxial $\text{La}_{0.67}\text{Ca}_{0.33}\text{MnO}_3$ (LCMO) thin films [2], 53% in $\text{La}_{0.8}\text{Sr}_{0.2}\text{MnO}_3$ at 5 T and 260 K [6]. It is a considerable important issue, for potential applications and for microscopic understanding, to resolve what

principal factors determine the Curie temperature and the magnetoresistance. It was proposed that in doped magnetic compounds the mixed $\text{Mn}^{3+}/\text{Mn}^{4+}$ valence give rise to both ferromagnetism and metallic behavior [7,8]. Earlier studies [9,10] showed that the mixed $\text{Mn}^{3+}/\text{Mn}^{4+}$ ratio could be changed by changing the doping level and by varying the oxygen content. According to mean-field theory [11,12], the presence of species with different ionic radii can change the lattice parameters and also lead to a shift in the Curie temperature. In fact, Jin et al. [13] reported first that CMR could be improved in sintered bulk samples of $\text{La}_{0.60}\text{Y}_{0.07}\text{Ca}_{0.33}\text{MnO}_3$. Some investigations [14–17] also present detailed results of manganese perovskites by substituting different doping level of Y, Pr, and Nd for La. These results indicate that there is considerable coupling between magnetism and the lattice strain in this system. Here we report the CMR behavior of a series of $(\text{La}_{1-x}\text{Gd}_x)_{0.67}\text{Ca}_{0.33}\text{MnO}_3$ (LGCMO) samples. The temperature dependence of electric and the magnetization properties are also examined. We find that these properties depend on the concentration of gadolinium. The MR value of the LGCMO system for $x \sim 0.3$ reaches approximately 92.5% in a low applied magnetic field, typically near $B = 0.85$ T.

* Corresponding author. Present address: Department of Chemistry, University of Guelph, Guelph, Ont., Canada N1G 2W1.

2. Experimental

We prepared a series of $(\text{La}_{1-x}\text{Gd}_x)_{0.67}\text{Ca}_{0.33}\text{MnO}_3$ ($x = 0.10, 0.20, 0.30, 0.40$, and 1.00) samples using the

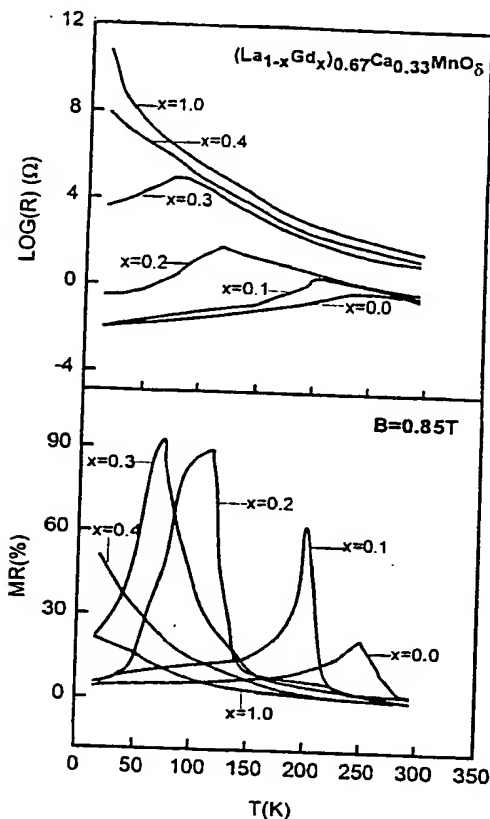


Fig. 1. Temperature dependence of the resistance (top panel) and magnetoresistance $\text{MR} [(R_0 - R_B)/R_0]$ (bottom panel) for a series of samples $(\text{La}_{1-x}\text{Gd}_x)_{0.67}\text{Ca}_{0.33}\text{MnO}_3$; x values are labeled on the graph.

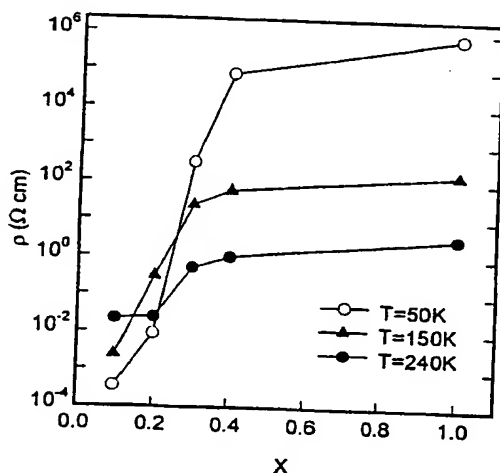


Fig. 2. Change of the resistivity taken at 50, 150 and 240 K as a function of gadolinium composition for $(\text{La}_{1-x}\text{Gd}_x)_{0.67}\text{Ca}_{0.33}\text{MnO}_3$ series.

solid-state reaction method. Stoichiometric amounts of La_2O_3 , Gd_2O_3 , CaCO_3 , and MnO_2 were thoroughly mixed, and calcined at 1000°C for 8 h in air. The calcined materials were ground again, pressed into small disks, and sintered at 1420°C for 8 h in oxygen atmosphere, and then cooled slowly to room temperature. The morphology and chemical composition of the sintered samples were checked by scanning electron microscope (SEM) and energy-dispersive spectroscopy (EDS), and X-ray diffraction (XRD) analysis was performed. The electric resistance and magnetoresistance of the samples were measured by a standard four-point contact technique in the temperature range of 12–300 K, and magnetic field $B \leq 0.85 \text{ T}$. For highly resistive samples, the resistance measurements were carried out with a high impedance electrometer. The magnetization of the samples was measured by a vibrating sample magnetometer (VSM).

3. Results and discussion

Fig. 1 represents the temperature dependence characteristics of the resistance R , the MR ratio with $(R_0 - R_B)/R_0$ for six samples of $x = 0.0, 0.1, 0.2, 0.3, 0.4$, and 1.0 . It is evident that all samples except the ones with $x = 0.4$ and 1.0 show a semiconductor-metal transition, while semiconductor behavior (i.e. a negative dR/dT) occurs above the peak temperature and metallic behavior (i.e. a positive dR/dT) below. The temperature of maximum magnetoresistance is almost located in the metallic-behavior region on the low temperature side of the resistivity peak. Clearly the peak temperature T_c and MR ratio shift are associated with an increased gadolinium composition. It is interesting to note that T_c decreases from 205 to 75 K and MR peak value increases as the value of x increases from 0.1 to 0.3, which is similar to the results in Y-doping samples [14,15]. At $T = 72 \text{ K}$, the highest MR value of about 92.5% is observed for the $x = 0.3$ sample at $B = 0.85 \text{ T}$. Such a low field MR behavior in our measurement is of much importance for many magnetic field sensor application.

Fig. 2 gives the doping level dependence of the resistivity measured at temperatures $T = 50, 150$ and 240 K . It can be seen that the resistivity increases rapidly with increasing doping level x at several temperature points. The results in Fig. 1 and Fig. 2 suggest that the high resistivity in polycrystalline series is associated with large magnetoresistance values at measured temperature ranges.

The magnetization of samples as a function of temperature is shown in Fig. 3. With increasing the gadolinium content x , the magnitude of the saturation

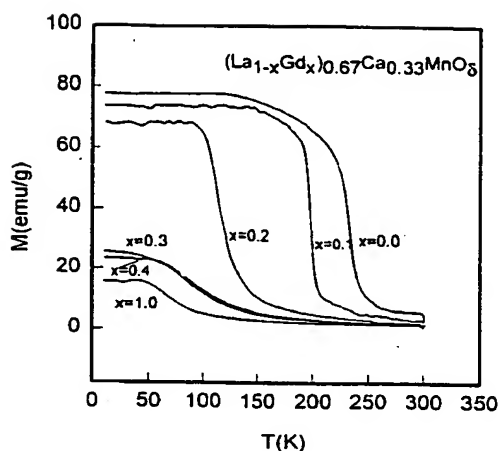


Fig. 3. Temperature dependence of the magnetization for samples of the series $(\text{La}_{1-x}\text{Gd}_x)_{0.67}\text{Ca}_{0.33}\text{MnO}_5$ at 10 kGs measured on cooling.

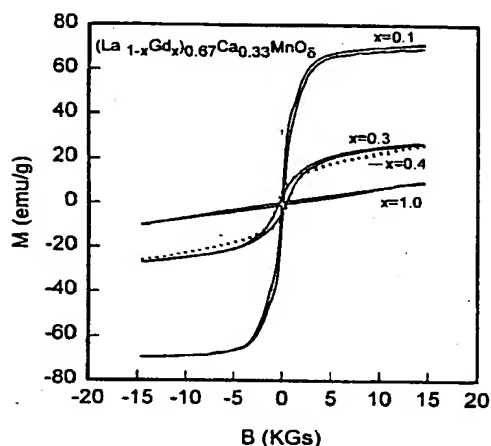


Fig. 4. Magnetization curves of $(\text{La}_{1-x}\text{Gd}_x)_{0.67}\text{Ca}_{0.33}\text{MnO}_5$ series at 10 K as a function of magnetic field.

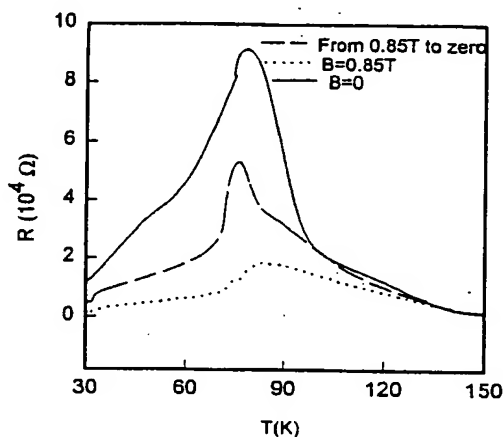


Fig. 5. Temperature dependence of the resistance for a $(\text{La}_{0.7}\text{Gd}_{0.3})_{0.67}\text{Ca}_{0.33}\text{MnO}_5$ sample with different magnetic histories.

magnetization is severely depressed. It may also be noted from Fig. 3 that the ferromagnetic transition becomes very broad for higher Gd content. Since a sharp transition may not exist in most of these Gd-doped polycrystalline ceramics, the general Arrott plot method or similar approach is not appropriate to determine the Curie temperature of these samples. We determined the Curie temperatures by an extrapolation procedure described by Leung et al. [18]. The obtained points by this method coincide approximately with the above transition temperatures in Fig. 1.

The magnetization curves up to 15 kGs at temperature of 10 K for several samples of $x = 0.1, 0.3, 0.4$, and 1.0 are shown in Fig. 4. With increasing x , the smaller saturation magnetization and the higher saturation field can be observed, indicating the MR value may be larger at higher fields for the samples with optimum doping level.

Xiong et al. [19] reported on a novel magnetoresistive memory effect in the $\text{Nd}_{0.7}\text{Sr}_{0.3}\text{MnO}_2$ films. The resistivity of the film depends not only on the applied magnetic field but also on the magnetic history. In the systematic study of CMR in several LGCMO samples, we have also observed a CMR memory effect in some of Gd-doped LCMO samples. Fig. 5 shows the temperature dependence of the resistance for a LGCMO sample ($x = 0.3$) with different magnetic histories. One notices that when the field is reduced to zero, the remanent resistance is not recovered to the original zero-field value. It is also noteworthy that the obvious difference between curves of the remanent resistance and original zero-field resistance occurs over a wide temperature ranges, below and near the transition temperature T_c . At T well above T_c , the curve of the remanent resistance tends to values of the original zero-field resistance.

A more systematic investigation of these manganites has shown that two factors govern the CMR properties of these materials, the size of the interpolated cation and the hole carrier density. The first factor influences dramatically the Mn–Mn distance and consequently the overlapping of the manganese–oxygen orbitals. The hole carrier density is controlled by the $\text{Mn}^{3+}/\text{Mn}^{4+}$ ratio, depending on the charge of the interpolated cations. Since the $\text{Mn}^{3+}/\text{Mn}^{4+}$ ratio remained fixed at 7/3 in our $(\text{La}_{1-x}\text{Gd}_x)_{0.67}\text{Ca}_{0.33}\text{MnO}_5$ samples, the effect of Gd doping in polycrystalline LCMO material on their electrical and magnetic properties may be caused by ionic radii difference between trivalent lanthanum and gadolinium (the ionic radius of La^{3+} is 1.22 Å, and that of Gd^{3+} is 1.11 Å). It has also been reported that LCMO was a nearly cubic perovskite structure [20] while $(\text{Gd}_{1-x}\text{Ca}_x)\text{MnO}_5$ was the orthorhombic [21]. With increasing doping level, it can be expected that the crystallographic structure changes gradually from cubic perovskite to orthorhombic, and the lattice constants

become smaller for larger x . The change in lattice parameter and crystallographic structure would affect the Mn–O–Mn bond angle, and canting of the Mn ion moment, and result in changes of the Mn–Mn electronic hopping parameter. This effect has been observed in the earlier studied $(\text{La}_{1-x}\text{Y}_x)_{0.67}\text{Ca}_{0.33}\text{MnO}_\delta$ and $(\text{La}_{1-x}\text{Pr}_x)_{0.67}\text{Ca}_{0.33}\text{MnO}_\delta$ systems [15–17].

In a cubic perovskite ABO_3 structure, the structural stability follows the perovskite tolerance factor $t = (r_A + r_O)/(\sqrt{2}(r_B + r_O))$, where r_A , r_B , and r_O represent the ionic radii of the lanthanide site, transition metal, and oxygen, respectively. For a perfect cubic perovskite structures, $t \approx 1$, while the Mn–O–Mn bond angle θ would be 180° . Due to the substitution of Gd in the system LCMO, there are three types of average A–O bond lengths corresponding to $A = \text{La}$, Ca and Gd , and two average B–O bond lengths corresponding to Mn ion in two oxidation states (Mn^{3+} and Mn^{4+}). It could be calculated to know that both the average ionic radius of A site $\langle r_A \rangle$ and the tolerance factor t decrease with increasing Gd doping level x . For $t < 1$, rather than a simple contraction of bond distances, the octahedra tilt and rotate to reduce the excess space around the A site, resulting in $\theta < 180^\circ$, thereby reducing the matrix element b , which described electron hopping between Mn sites [14]. Also, the increased bending of the Mn–O–Mn bond should induce the enhancement of the carrier effective mass or the narrowing of the bandwidth [17]. Thus, these changes arising from substitution by Gd will result in a decrease in T_c , and also produce a modification of the spin state of neighboring sites, thereby changing the electronic transport properties and associated properties. When decreasing the Mn–O–Mn bond angle more, the transport properties of LGCMO perovskites will remain nonmetallic to lowest temperatures. The results have been confirmed for our samples of LGCMO ($x \geq 0.4$) as shown in Fig. 1.

4. Conclusion

We have shown that the electric transport and magnetic behaviors of polycrystalline samples of $(\text{La}_{1-x}\text{Gd}_x)_{0.67}\text{Ca}_{0.33}\text{MnO}_\delta$ ($x \leq 1$) systematically varied by

changing the Gd doping level x . With increasing x , the MR ratio near T_c increases, and the T_c decreases. The maximum MR value of 92.5% is observed for $x = 0.3$ at $B = 0.85$ T. These results are attributed to the change in the lattice parameter.

Acknowledgements

This work was partially supported by National Science Foundation of China and Hong Kong RGC.

References

- [1] G.H. Jonker, J.H. van Saten, *Physica* 16 (1950) 337.
- [2] S. Jin, T.H. Tiefel, M. McCormack, R.A. Fastnacht, R. Ramesh, L.H. Chen, *Science* 264 (1994) 413.
- [3] H.S. Wang, Q. Li, K. Liu, C.L. Chien, *Appl. Phys. Lett.* 74 (1999) 2212.
- [4] R. von Helmolt, J. Wecker, B. Holzapfel, L. Schultz, K. Samwer, *Phys. Rev. Lett.* 71 (1993) 2331.
- [5] A. Urushibara, Y. Moritomo, T. Arima, A. Asamitsu, G. Kido, Y. Tokura, *Phys. Rev. B* 51 (1995) 14103.
- [6] H.J. Ju, C. Kwon, Q. Li, R.L. Greene, T. Vantakeson, *Appl. Phys. Lett.* 65 (1994) 2108.
- [7] C. Zener, *Phys. Rev.* 82 (1951) 403.
- [8] P.G. de Gennes, *Phys. Rev.* 118 (1960) 141.
- [9] G.C. Xiong, Q. Li, H.L. Ju, R.L. Greene, T. Venkatesan, *Appl. Phys. Lett.* 66 (1995) 1689.
- [10] R. von Helmolt, J. Wecker, K. Samwer, L. Haupt, K. Barner, J. *Appl. Phys.* 76 (1994) 6925.
- [11] T.H. Jacobs, K.H.J. Buschow, G.F. Zhou, X. Li, F.R. de Boer, *J. Magn. Magn. Mater.* 116 (1992) 220.
- [12] H. Sun, J.M.D. Coey, Y. Otani, D.P.F. Hurley, *J. Phys. Condens. Matter* 2 (1990) 6465.
- [13] S. Jin, H.M. O'Bryan, T.H. Tiefel, M. McCormack, W.W. Rhodes, *Appl. Phys. Lett.* 66 (1995) 382.
- [14] H.Y. Hwang, S.-W. Cheong, P.G. Radaelli, M. Marzino, B. Batlogg, *Phys. Rev. Lett.* 75 (1995) 914.
- [15] Z. Li, X.T. Zeng, H.K. Wong, *J. Appl. Phys.* 79 (1996) 5188.
- [16] W. Zhang, I.W. Boyd, M. Elliott, W. Herrenden-Harkerand, *Appl. Phys. Lett.* 69 (1996) 3599.
- [17] Z.B. Guo, N. Zhang, W.P. Ding, W. Yang, J.R. Zhang, Y.W. Du, *Solid State Commun.* 100 (1996) 769.
- [18] L.K. Leung, A.H. Morrish, C.W. Searle, *Can. J. Phys.* 47 (1969) 2697.
- [19] G.C. Xiong, Q. Li, H.L. Ju, S.M. Bhagat, S.E. Lofland, R.L. Greene, T. Venkatesan, *Appl. Phys. Lett.* 67 (1995) 3031.
- [20] J.B. Goodenough, *Prog. Solid State Chem.* 5 (1971) 145.
- [21] H. Taguchi, M. Nagao, M. Shimada, *J. Solid State Chem.* 82 (1989) 8.